



http://pubs.acs.org/journal/acsodf Article

# Short DNA Oligonucleotide as a Ag<sup>+</sup> Binding Detector

Fusheng Shen, Song Mao, Johnsi Mathivanan, Ying Wu, Arun Richard Chandrasekaran, Hehua Liu, Jianhua Gan,\* and Jia Sheng\*



Cite This: ACS Omega 2020, 5, 28565-28570



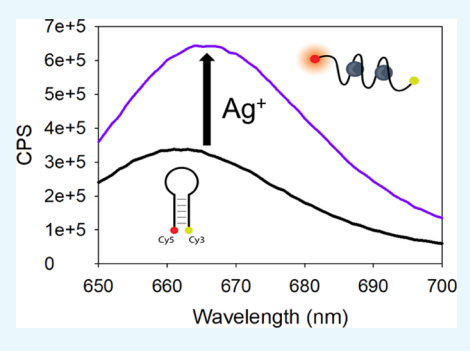
**ACCESS** 

Metrics & More

Article Recommendations

s Supporting Information

**ABSTRACT:** Ag<sup>+</sup> has been known to mediate several natural metallo-base pairs. Based on the unique structural information of a short 8-mer DNA strand (5′-GCACGCGC-3′) induced by Ag<sup>+</sup>, we constructed several fluorescent DNA beacons for the detection of Ag<sup>+</sup> according to the increase in the fluorescence emission on Ag<sup>+</sup> binding. This Ag<sup>+</sup> detection assay is quick, sensitive, and easy to adapt and can function in a wide range of temperatures from 5 to 65 °C.



## INTRODUCTION

Silver ions (Ag<sup>+</sup>) have been known as one of the most hazardous metal pollutants that can be widely distributed in air, water, soil, and even food. <sup>1-4</sup> The interaction of Ag<sup>+</sup> with various metabolites and inactivating sulfhydryl enzymes can cause cytopathic effects in many types of cells including keratinocytes, human tissue mast cells, human gingival fibroblasts, and endothelial cells. <sup>5-7</sup> Therefore, developing a sensitive and specific method to detect Ag<sup>+</sup> is important. Traditional methods for the detection of Ag<sup>+</sup> such as atomic absorption spectrometry (AAS), <sup>8,9</sup> inductively coupled plasmamass spectrometry (ICP-MS), <sup>10-12</sup> and ionic selective electrode (ISE) <sup>13</sup> are expensive and complex. <sup>14</sup> Hence, the need for a rapid and simple method for the detection of Ag<sup>+</sup> is significant.

Recently, the high specific interaction between nucleic acid bases and metal ions has been applied in metal ion detection.<sup>14</sup> Structural diversity plays a significant role in the physiological functions of DNA and biological processes such as gene metabolism and regulation,<sup>15</sup> as well as in nanotechnology.<sup>16</sup> Apart from the "usual" duplex and hairpin structures, DNA can also form triplexes and quadruplexes. <sup>17,18</sup> In most cases, these structures are stabilized by the pairing interactions of the nucleobases. It has been widely known that Watson-Crick, Wobble, and Hoogsteen base pairings can regulate these structures. Furthermore, DNA can also form metallo-base pairs in the presence of metal ions. Metallo-base pairs were first discovered in the early 1960s, 19 and they became a hot topic due to their significance in the development of novel therapeutics<sup>20-23</sup> and genetic code extension. <sup>24,25</sup> They also play a critical role in the design of functional materials including molecular magnets, 26-28 electrical transport nanoand other DNA-based nanodevices. 32-34 Metallobase pairs can be formed by both natural and artificial nucleobases. However, metallo-base pairs formed by natural nucleobases are more attractive due to the lower cost and simple synthesis even though they can be formed by artificial nucleobases as well. He was metal ions can interact with DNA in different ways. For example, Hg<sup>2+</sup> and Ag<sup>+</sup> interact with the bases of DNA. Meanwhile, Co<sup>2+</sup>, Ni<sup>2+</sup>, Mn<sup>2+</sup>, Zn<sup>2+</sup>, Cd<sup>2+</sup>, Pb<sup>2+</sup>, Cu<sup>2+</sup>, and Au<sup>3+</sup> can all interact with both the base and phosphate backbone portions of DNA.

In our previous work, we reported a non-helical DNA crystal structure with a new folding mode composed by a short 8-mer strand (5'-GCACGCGC-3') and Ag+ (Figure 1A) with negative peaks near 220 and 280 nm in the CD spectrum.<sup>34</sup> This 8-mer strand has also been reported as a machine learning designed oligomer to stabilize a fluorescent DNA-based silver cluster by Copp et al., 40 which points to something exceptional about the properties of this sequence. In this structure, two Ag+ ions mediated the pairing between the two G7 and the two C8 residues in the 3' terminus.34 Based on this specific structural conformation and the regularly used molecular beacon platform, 34,41 we designed three fluorescent DNA beacons for the detection of Ag<sup>+</sup> (Table 1 and Figure 1B). As shown in Table 1, the Ag+-binding sequence is located at the stem position in the first oligonucleotide (DNA1) and at the loop positions with a partial presence on the stem in the other two oligonucleotides (DNA2 and DNA3). The 8-mer sequence

Received: July 14, 2020 Accepted: October 14, 2020 Published: October 28, 2020





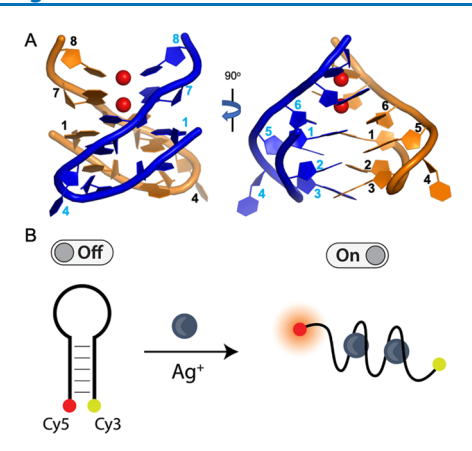


**Figure 1.** (A) Overall structure of the (5'-GCACGCGC-3') and Ag<sup>+</sup> complex. Ag<sup>+</sup> ions are shown as red spheres. DNA strands are shown as cartoons in yellow and blue for strand A and strand B, respectively. (B) Ag<sup>+</sup>-specific binding assays for the designed DNA

Table 1. Designed DNA Sequence Information

Entry	Sequence
DNA1	5'-/Cy5/GCACGCGCTTTTGCACGCGC/Cy3Sp/-3'
DNA2	5'-/Cy5/TTTTTGCACGCGCAAAAA/Cy3Sp/-3'
DNA3	5'-/Cy5/(TTTTT) <sub>2</sub> GCACGCGC(AAAAA) <sub>2</sub> /Cy3Sp/-3'

(5'-GCACGCGC-3') in DNA1 is a "near complement" that can form a hairpin structure at low temperatures. In each version, we attached a fluorophore group on both ends of the strands (a Cy5 and a Cy3). All of the designed oligonucleotides form stem loop structures without Ag<sup>+</sup> ions. In this initial "off" state, the Cy5 and Cy3 are close to each other in the hairpin structure, showing minimal fluorescence due to the quenching effects. <sup>42,43</sup> The presence of Ag<sup>+</sup> induces a new folding mode ("on" state), causing the Cy5 and Cy3 to be separated, thus causing an increase in fluorescence. The addition of Ag<sup>+</sup> causes a dose-dependent increase in fluorescence emission on our designed DNA oligonucleotides (DNA1 and DNA2), enabling measurement of Ag<sup>+</sup> levels.

# ■ RESULTS AND DISCUSSION

Our first step was to optimize the concentrations of DNA and  $Ag^+$  to be used for the assay. Using a fluorimeter, we measured the detection limit of  $Ag^+$  using DNA1 to be 100 pM at 25 °C (Figure S1), and the fluorescence signal saturated at 500 pM  $Ag^+$ . The fluorescence signal due to the effect of  $Ag^+$  on both DNA1 and DNA2 was only observable when we used a DNA

concentration of 1 nM, and the fluorescence of both oligonucleotides showed obvious increase after adding 5 equiv of  $\mathrm{Ag}^+$ . Since the increase in fluorescence was relatively small at the DNA concentration of 1 nM, we used 100 nM DNA solution for our fluorescence assays.

We then tested the temperature effect on the fluorescence of DNA1 and DNA2 without the addition of Ag<sup>+</sup>. Figure 2 shows the excitation of both DNA1 and DNA 2 with 470 nm wavelength, which generated two fluorescence emission bands, one belongs to Cy3 emission (~570 nm), and the other belongs to Cy5 emission (~660 nm). These spectra indicate that there is a FRET between Cy3 (donor) and Cy5 (acceptor) in all cases with varying efficiencies. The results suggest that increasing the temperature of both DNA strands (DNA1 and DNA2) decreases the FRET efficiency, which is observed by a greater decrease in Cy5 emission with respect to the Cy3 one. Particularly, the effect of temperature on the unfolding of DNA2 is observed to be more dramatic, which is observed by a smaller Cy5/Cy3 emission ratio at a higher temperature. The full fluorescence spectra (Figure 3) shows

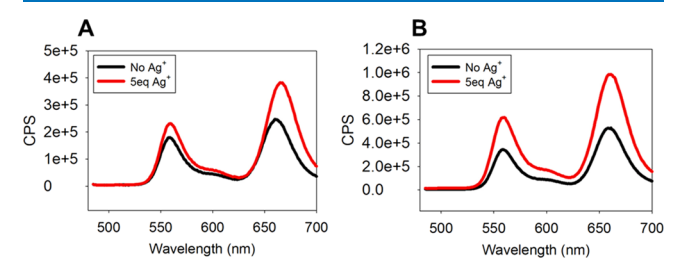
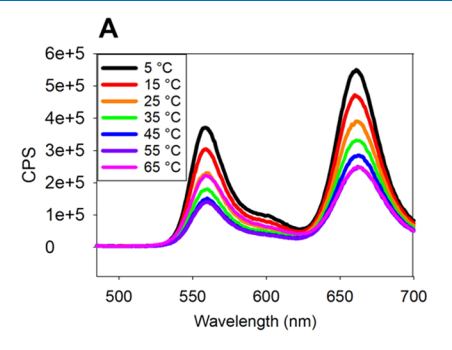


Figure 3. Emission spectra of (A) DNA1 and (B) DNA2 with and without 5 equiv of  $Ag^+$  at 5 °C.

that both Cy3 and Cy5 emission of both DNA1 and DNA2 are enhanced with the addition of Ag<sup>+</sup> as compared to the ones without Ag<sup>+</sup> at 5 °C. Meanwhile, we would expect that some contact quenching effect should suppress Cy3 and Cy5 fluorescence without Ag+ in the "off" state, and when Ag+ is added into the solution, the dyes will separate and "light up" in the "on" state; since FRET is occurring in this system for some fraction of fluorophore pairs, the fluorescence of Cy5 would also be enhanced by the closer proximity to Cy3. These competing effects of possible collisional quenching and FRET enhancing would be difficult to untangle for detailed mechanistic studies and precise quantitative calculations of binding constants. Therefore, the binding interactions of Ag<sup>+</sup> ions with the DNA could only be measured qualitatively using the integrated fluorescence changes as shown in the following sections.



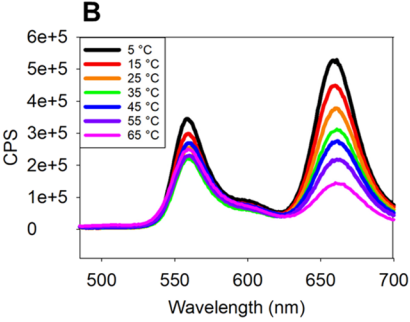


Figure 2. Emission spectra of (A) DNA1 and (B) DNA2 at different temperatures.

In addition, Figure 2 also shows the fluorescence signal decreased with the increased temperatures for both DNA1 and DNA2 alone, and both strands exhibited the highest fluorescence at 5 °C. This trend is consistent with the previous literature that reported decrease in fluorescence of Cy5 as temperature increases. He for DNA1, when the temperature reached 55 °C, increasing the temperature did not affect the fluorescence any more. However, DNA2 showed the lowest fluorescence signal at 65 °C. Therefore, we designed further experiments with temperatures ranging from 5 to 55 °C for DNA1 and 5 to 65 °C for DNA2 to calculate the binding constants.

We measured the binding constants  $(K_d)$  for both DNA1 and DNA2 with  $Ag^+$  by fluorescent titration at different temperatures. The measurement is enabled by the dose-dependent increase in fluorescence emission at 660 nm (the emission wavelength of Cy5) caused by the interaction of  $Ag^+$  with the 5'-Cy5- and 3'-Cy3-labeled DNA oligonucleotides. DNA1 and DNA2 showed slightly different binding constants at different temperatures, calculated from the middle points of their binding curves with  $Ag^+$  (Table 2). For DNA1, the

Table 2. Sequences and Binding Constants of the Designed Fluorescent DNA Probes

entry	binding constant $(K_d)^a$
DNA1	175.4 nM (5 °C)
	143.3 nM (25 °C)
	150.1 nM (37 °C)
	187.3 nM (45 °C)
	125.6 nM (55 °C)
DNA2	81.2 nM (5 °C)
	75.6 nM (25 °C)
	72.4 nM (37 °C)
	31.3 nM (50 °C)
	55.3 nM (65 °C)

<sup>a</sup>The binding constants were measured in 7.5 mM MOPS +2.5 mM NaCl (pH 7.2).

strongest binding occurred at 55 °C, and the weakest binding happened at 45 °C. Meanwhile, DNA2 exhibited the strongest binding at 50 °C and the weakest binding at 5 °C.

In our binding assays of DNA1, temperature played an important role (Figure 4). At 5, 25, and 37 °C, the saturated concentrations of Ag<sup>+</sup> were all ~250 nM, which is 2.5 equiv of DNA1 solution (shown in Figure 4C and Figures S2 and S3). Meanwhile, at 45 °C, the saturated concentration of Ag<sup>+</sup> was 300–350 nM (Figure S4). However, at 55 °C, the saturated concentration of Ag<sup>+</sup> was only 200 nM (Figure 4D). As listed in Table 2, DNA1 exhibited strong and similar binding affinities of  $K_d$  in 100–200 nM at all temperatures. We also found that the fluorescence increased by almost twofold at all temperatures, showing that increase in temperature does not affect the conformation of the Ag<sup>+</sup> and DNA complex. Another interesting discovery is that the highest binding affinity ( $K_d$  = 125.6 nM) occurred at the highest temperature (55 °C).

Temperature also played an important role for DNA2. At 5 and 65 °C, the saturated concentrations of  $Ag^+$  were 150 and 200 nM, respectively (Figure 5). Meanwhile, at other temperatures (25, 37, and 50 °C), the saturated concentrations of  $Ag^+$  were all 100 nM, which equals the amount of our DNA2 solution (Figures S5–S7). In addition, DNA2 exhibited the highest binding affinity with  $K_d = 31.3$  nM at 50 °C. When

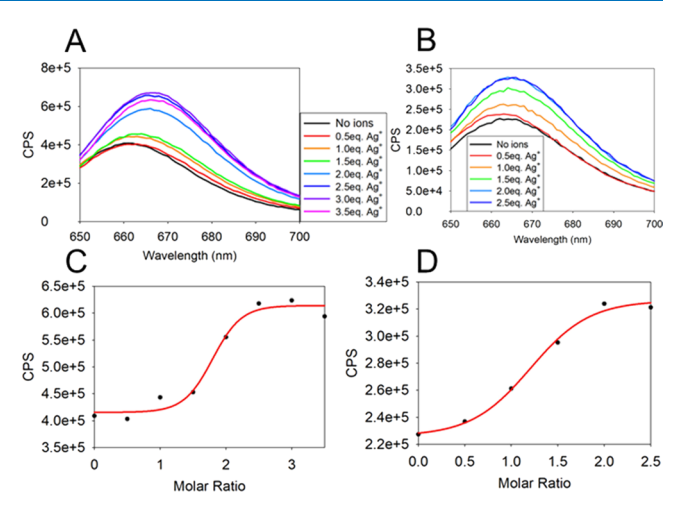


**Figure 4.** Emission spectra of  $Ag^+$  titration with DNA1 at (A) 5 °C and (B) 55 °C. Binding curves of DNA1 with  $Ag^+$  at (C) 5 °C and (D) 55 °C.

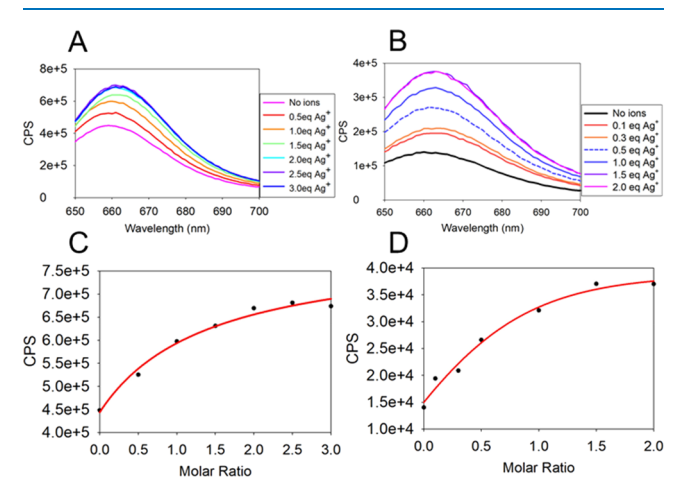


**Figure 5.** Emission spectra of  $Ag^+$  titration with DNA2 at (A) 5 °C and (B) 65 °C. Binding curves of DNA2 with  $Ag^+$  at (C) 5 °C and (D) 65 °C.

the temperature was decreased to 5  $^{\circ}$ C,  $K_{\rm d}$  was 81.2 nM, which was almost threefold of  $K_{\rm d}$  at 50 °C (Table 2). Binding constants listed for 5, 25, 37, 50, and 65 °C in Table 2 showed that the binding constants decreased with increased temperature except 65 °C, which means that increasing titration temperature makes the interaction between Ag<sup>+</sup> and DNA2 stronger. We also noticed that the fluorescence was increased by almost fourfold at 65 °C but only less than twofold at other temperatures. The circular dichroism (CD) spectrum of DNA2 (no ions) at 5 and 65 °C (shown in black lines of Figure S11) indicates that the hairpin of DNA2 does not open up at 65 °C, which confirms that binding with Ag+ changes the conformation of DNA2 more at a higher temperature. The comparison of all the binding constants of DNA1 and DNA2 shows that DNA2 exhibits onefold higher binding affinity with Ag<sup>+</sup> than DNA1.

To elucidate the effect of Ag<sup>+</sup>, another DNA sequence (DNA3) with more A–T base pairs (10 nt) at the end of the strand was designed. As shown in Figure 6, at room temperature, DNA3 exhibited very low fluorescence without Ag<sup>+</sup>, due to the very close distance between the two

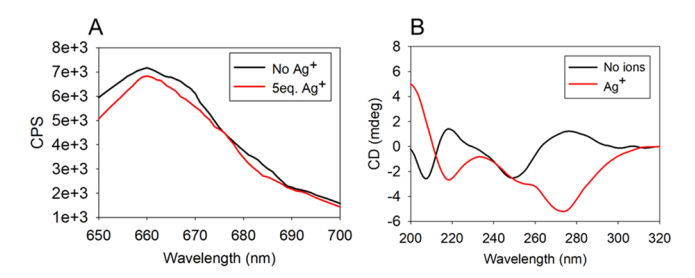


**Figure 6.** (A) Emission spectra and (B) CD spectra of DNA3 with 5 equiv of Ag<sup>+</sup> at 25 °C.

fluorophores Cy3 and Cy5. Interestingly, the fluorescence of DNA3 did not increase after adding 5 equiv of Ag<sup>+</sup>.

However, CD spectra showed the specific negative peak around 280 nm after the addition of  $Ag^+$  (Figure 6B), indicating the formation of the new folding mode of DNA3. Depending on this observation, we concluded that the structural conformational change in the middle of DNA3 is not strong enough to separate terminal Cy3 and Cy5 with 10 A-T base pairs.

For DNA1 and DNA2, the result of fluorescent titration indicated that the saturation concentration of Ag+ is from 100 to 350 nM. Therefore, we used 500 nM Ag<sup>+</sup> and 100 nM of DNA oligonucleotides for the specificity assay. Since Pb<sup>2+</sup>, Ni<sup>2+</sup>, Cu<sup>2+</sup>, and Fe<sup>3+</sup> have been reported to mediate metallobase pairs in different ways,<sup>35</sup> we applied our assay on these metal ions. We used a fluorimeter to test DNA1 and DNA2 and found that there was no obvious increase in fluorescence after adding 500 nM Pb<sup>2+</sup>, Ni<sup>2+</sup>, Cu<sup>2+</sup>, and Fe<sup>3+</sup> at low (5 °C) and high temperatures (55 or 65 °C) (Figures S8 and S10). However, there was a dramatic increase in fluorescence by adding 500 nM Ag<sup>+</sup>. Together with the CD spectra at different temperatures shown in Figures S9 and S11, we established that our designed DNA oligonucleotides exhibited a specific binding mode only after binding with Ag<sup>+</sup>. In the CD spectra in Figures S9 and S11, there is a positive peak near 280 nm and a negative peak near 240 nm for both DNA1 and DNA2 before the addition of Ag+, indicating that both of them are in a typical B-form structure. 16 However, after adding Ag+, there were negative peaks near 220 and 280 nm, which is consistent with our previous results.<sup>34</sup> In addition, the  $T_{\rm m}$  results shown in Figure S12 also indicate that the stable duplex conformation of DNA1 and DNA2 were destroyed after adding Ag+. Therefore, based on the circular dichroism and  $T_{\rm m}$  results, we confirmed our hypothesis that the increase in fluorescence after the addition of Ag+ is due to the non-helical conformation of the designed DNA oligonucleotides. Secondary structure analysis of all three probe sequences is provided in Figure S13.

To further confirm our hypothesis, another fluorescent DNA beacon was designed by placing a 5'-fluorophore (Cy5) and 3'-quencher (BHQ-2) at the end of DNA1' (5'-/Cy5/GCACGCGCTTTTGCACGCGC/BHQ-2/-3'). As shown in Figure S14, the fluorescence of DNA1' was increased by adding Ag<sup>+</sup>, which means that our hypothesis was also confirmed by using another designed DNA beacon. However, the detection limitation of DNA1' was 5  $\mu$ M, which is much less sensitive than that (5 nM) of DNA1 (5'-/Cy5/GCACGCGCTTTTGCACGCGC/Cy3Sp/-3').

Based on our previous paper and recent data, Ag<sup>+</sup> specifically binds to G-G and C-C in our designed DNA oligonucleotides.<sup>34</sup> It has been reported that Ag<sup>+</sup> specifically bound with C-C in a molar ratio of 1:1 with a binding constant in a

micromolar range.<sup>45</sup> For our designed sequences, all of the binding constants at different temperatures are in the 30-190 nM range. Our method allows Ag<sup>+</sup> to be detected in 5-500 nM, while the detection range of a newly reported fluorescence biosensor based on exonuclease III enzymatic amplification is 5-1500 pM.<sup>14</sup> However, compared to our simple and rapid detection method, the Ag+ analysis based on enzymatic amplification<sup>14</sup> is more time consuming, expensive, and requires more skilled technicians. In addition, the molar ratio was approximately 1:1 to 3:1, which may be due to our designed oligonucleotides containing both G-G and C-C base pairs. Different from previous C-Ag<sup>+</sup>-C and G-Ag<sup>+</sup>-G reports,  $^{45,46}$  our  $T_{\rm m}$  and CD results revealed the formation of non-helical conformation after adding Ag+. In addition, temperature-dependent K<sub>d</sub> measurements reveal that our designed DNA oligonucleotides exhibit a high binding affinity with Ag<sup>+</sup> at both low temperature (5 °C) and high temperature (65 °C).

## CONCLUSION

In summary, we report the use of a fluorescent beacon to detect Ag+ with high affinity and specificity. All the three designed DNA oligonucleotides exhibit a specific and modest to high binding affinity  $(K_d)$  in the nanomolar range with  $Ag^+$ . Although the binding constants measured in this system might not be precisely quantitative due to the intrinsic complicated mechanism of fluorescence change determined by the competing effects between collisional quenching and FRET enhancing effects of the two dyes we used, these DNA oligonucleotides provide a highly sensitive, simple, and quick route for the detection of Ag+ ions. Further, this detection method can work at various temperatures. More systematic and thorough biophysical, structural, and molecular dynamics simulation work will be necessary to elucidate the detailed working mechanisms for the further optimization of this system.

## ■ GENERAL EXPERIMENTAL SECTION

**DNA Oligonucleotides.** DNA oligonucleotides were synthesized by IDT (integrated DNA technology).

Melting Temperature Measurements. A Varian CARY 1 spectrophotometer equipped with a Peltier temperature controller was used to obtain UV–vis thermal denaturation data. DNA samples (1.5  $\mu$ M) were prepared in 7.5 mM MOPS and 2.5 mM Na<sup>+</sup> buffer (pH 7.2). Before the  $T_{\rm m}$  studies, DNA samples were heated to 85 °C for 5 min, slowly cooling to room temperature, and placed at 4 °C overnight. The following step was adding 5 equiv of AgNO<sub>3</sub>, Pb(NO<sub>3</sub>)<sub>2</sub>, NiCl<sub>2</sub>, CuCl<sub>2</sub>, or FeCl<sub>3</sub> for the melting temperature study.

**Secondary Structural Studies.** A J-815 CD spectrometer was used to obtain all the CD spectra. DNA samples (5  $\mu$ M) are prepared in 7.5 mM MOPS and 2.5 mM Na<sup>+</sup> buffer (pH 7.2). Before checking CD spectra, DNA samples were heated to 85 °C for 5 min, slowly cooling to room temperature, and placed at 4 °C overnight. Finally, 5 equiv of AgNO<sub>3</sub>, Pb(NO<sub>3</sub>)<sub>2</sub>, NiCl<sub>2</sub>, CuCl<sub>2</sub>, or FeCl<sub>3</sub> was added.

**Fluorescence Studies.** A Horiba 3 Modular spectrofluorometer was used for all the fluorescent titrations and specificities study. DNA samples (100 nM) are prepared in 7.5 mM MOPS and 2.5 mM Na<sup>+</sup> buffer (pH 7.2). Before the experiments, DNA samples were heated to 85 °C for 5 min, slowly cooling to room temperature, and placed at 4 °C

overnight. AgNO<sub>3</sub>, Pb(NO<sub>3</sub>)<sub>2</sub>, NiCl<sub>2</sub>, CuCl<sub>2</sub>, and FeCl<sub>3</sub> were used in this study. Excitation wavelength is 470 nm.

**Binding Constant** ( $K_d$ ) **Studies.** The binding curves for both DNA1 and DNA2 with  $Ag^+$  were measured by fluorescent titration at different temperatures. The measurement is enabled by the dose-dependent increase in fluorescence emission at  $\sim 660$  nm (the emission wavelength of CyS) caused by the interaction of  $Ag^+$  with the 5'-CyS- and 3'-Cy3-labeled DNA oligonucleotides. Afterward, the binding constants ( $K_d$ ) for both DNA1 and DNA2 were calculated from the middle points of their binding curves in the presence of  $Ag^+$ .

#### ASSOCIATED CONTENT

# Supporting Information

The Supporting Information is available free of charge at https://pubs.acs.org/doi/10.1021/acsomega.0c03372.

Additional results (Figures S1-S13) and details of experimental methods (PDF)

# AUTHOR INFORMATION

## **Corresponding Authors**

Jianhua Gan — Shanghai Public Health Clinical Center, State Key Laboratory of Genetic Engineering, Collaborative Innovation Center of Genetics and Development, School of Life Sciences, Fudan University, Shanghai 200438, China; orcid.org/0000-0002-8438-8852; Phone: (86)21-3124-6543; Email: ganjhh@fudan.edu.cn

Jia Sheng — Department of Chemistry and The RNA Institute, University at Albany, State University of New York, Albany, New York 12222, United States; orcid.org/0000-0001-6198-390X; Phone: (1)518-437-4419; Email: jsheng@albany.edu

# Authors

Fusheng Shen – Department of Chemistry and The RNA Institute, University at Albany, State University of New York, Albany, New York 12222, United States

Song Mao – Department of Chemistry and The RNA Institute, University at Albany, State University of New York, Albany, New York 12222, United States

Johnsi Mathivanan – Department of Chemistry and The RNA Institute, University at Albany, State University of New York, Albany, New York 12222, United States

Ying Wu — Department of Chemistry and The RNA Institute, University at Albany, State University of New York, Albany, New York 12222, United States

Arun Richard Chandrasekaran — The RNA Institute, University at Albany, State University of New York, Albany, New York 12222, United States

Hehua Liu — Shanghai Public Health Clinical Center, State Key Laboratory of Genetic Engineering, Collaborative Innovation Center of Genetics and Development, School of Life Sciences, Fudan University, Shanghai 200438, China

Complete contact information is available at: https://pubs.acs.org/10.1021/acsomega.0c03372

## **Author Contributions**

The manuscript was written through contributions of all authors. / All authors have given approval to the final version of the manuscript. /.

#### **Notes**

The authors declare no competing financial interest.

#### ACKNOWLEDGMENTS

We are grateful to NSF (MCB-1715234) and the University at Albany, State University of New York for the financial support. We thank Prof. Mehmet Yigit and Prof. Maksim Royzen for the discussion.

## REFERENCES

- (1) Zhang, Y.; Li, H.; Xie, J.; Chen, M.; Zhang, D.; Pang, P.; Wang, H.; Wu, Z.; Yang, W. Electrochemical biosensor for silver ions based on amplification of DNA–Au bio–bar codes and silver enhancement. *J. Electroanal. Chem.* **2017**, 785, 117–124.
- (2) Zhang, Y.; Li, H.; Chen, M.; Fang, X.; Pang, P.; Wang, H.; Wu, Z.; Yang, W. Ultrasensitive electrochemical biosensor for silver ion based on magnetic nanoparticles labeling with hybridization chain reaction amplification strategy. *Sens. Actuators, B* **2017**, 249, 431–438.
- (3) Wang, G.; Wang, S.; Yan, C.; Bai, G.; Liu, Y. DNA-functionalized gold nanoparticle-based fluorescence polarization for the sensitive detection of silver ions. *Colloids Surf., B* **2018**, *167*, 150–155.
- (4) Miao, P.; Tang, Y.; Wang, L. DNA Modified Fe<sub>3</sub>O<sub>4</sub>@Au Magnetic Nanoparticles as Selective Probes for Simultaneous Detection of Heavy Metal Ions. *ACS Appl. Mater. Interfaces* **2017**, *9*, 3940–3947.
- (5) Zhou, W.; Ding, J.; Liu, J. 2-Aminopurine-modified DNA homopolymers for robust and sensitive detection of mercury and silver. *Biosens. Bioelectron.* **2017**, *87*, 171–177.
- (6) Gong, T.; Liu, J.; Liu, X.; Liu, J.; Xiang, J.; Wu, Y. A sensitive and selective sensing platform based on CdTe QDs in the presence of l-cysteine for detection of silver, mercury and copper ions in water and various drinks. *Food Chem.* **2016**, *213*, 306–312.
- (7) Poon, V. K. M.; Burd, A. In vitro cytotoxity of silver: implication for clinical wound care. *Burns* **2004**, *30*, 140–147.
- (8) López-López, J. A.; Jönsson, J. A.; García-Vargas, M.; Moreno, C. Simple hollow fiber liquid membrane based pre-concentration of silver for atomic absorption spectrometry. *Anal. Methods* **2014**, *6*, 1462–1467.
- (9) López-López, J. A.; Herce-Sesa, B.; Moreno, C. Solvent bar micro-extraction with graphite atomic absorption spectrometry for the determination of silver in ocean water. *Talanta* **2016**, *159*, 117–121.
- (10) Balcaen, L.; Bolea-Fernandez, E.; Resano, M.; Vanhaecke, F. Inductively coupled plasma Tandem mass spectrometry (ICP-MS/MS): A powerful and universal tool for the interference-free determination of (ultra)trace elements A tutorial review. *Anal. Chim. Acta* **2015**, 894, 7–19.
- (11) Sötebier, C. A.; Weidner, S. M.; Jakubowski, N.; Panne, U.; Bettmer, J. Separation and quantification of silver nanoparticles and silver ions using reversed phase high performance liquid chromatography coupled to inductively coupled plasma mass spectrometry in combination with isotope dilution analysis. *J. Chromatogr. A* **2016**, 1468, 102–108.
- (12) Ramos, K.; Ramos, L.; Gómez-Gómez, M. M. Simultaneous characterisation of silver nanoparticles and determination of dissolved silver in chicken meat subjected to in vitro human gastrointestinal digestion using single particle inductively coupled plasma mass spectrometry. *Food Chem.* **2017**, *221*, 822–828.
- (13) Lai, C.-Z.; Fierke, M. A.; da Costa, R. C.; Gladysz, J. A.; Stein, A.; Bühlmann, P. Highly Selective Detection of Silver in the Low ppt Range with Ion-Selective Electrodes Based on Ionophore-Doped Fluorous Membranes. *Anal. Chem.* **2010**, *82*, 7634–7640.
- (14) Li, Y.; Yuan, J.; Xu, Z. A Sensitive Fluorescence Biosensor for Silver Ions (Ag<sup>+</sup>) Detection Based on C-Ag<sup>+</sup>-C Structure and Exonuclease III-Assisted Dual-Recycling Amplification. *J. Anal. Methods Chem.* **2019**, 2019, 3712032.
- (15) Choi, J.; Majima, T. Conformational changes of non-B DNA. Chem. Soc. Rev. 2011, 40, 5893–5909.

- (16) Ng, W. D.; Wong, C. K. B. SELF-RECOGNITION OF DNA FROM LIFE PROCESSES TO DNA COMPUTATION. *Biophys. Rev. Lett.* **2007**, *02*, 123–137.
- (17) Kaushik, S.; Kaushik, M.; Svinarchuk, F.; Malvy, C.; Fermandjian, S.; Kukreti, S. Presence of Divalent Cation Is Not Mandatory for the Formation of Intramolecular Purine-Motif Triplex Containing Human c-jun Protooncogene Target. *Biochemistry* **2011**, *50*, 4132–4142.
- (18) Adrian, M.; Ang, D. J.; Lech, C. J.; Heddi, B.; Nicolas, A.; Phan, A. T. Structure and Conformational Dynamics of a Stacked Dimeric G-Quadruplex Formed by the Human CEB1 Minisatellite. *J. Am. Chem. Soc.* **2014**, *136*, 6297–6305.
- (19) Simpson, R. B. Association Constants of Methylmercuric and Mercuric Ions with Nucleosides. *J. Am. Chem. Soc.* **1964**, *86*, 2059–2065
- (20) Alvarez-Salas, L. M. Nucleic Acids as Therapeutic Agents. Curr. Top. Med. Chem. 2008, 8, 1379–1404.
- (21) Deleavey, G. F.; Damha, M. J. Designing Chemically Modified Oligonucleotides for Targeted Gene Silencing. *Chem. Biol.* **2012**, *19*, 937–954.
- (22) Schubert, S.; Kurreck, J. Ribozyme- and Deoxyribozyme-Strategies for Medical Applications. *Curr. Drug Targets* **2004**, *5*, 667–681.
- (23) Xing, H.; Wong, N. Y.; Xiang, Y.; Lu, Y. DNA aptamer functionalized nanomaterials for intracellular analysis, cancer cell imaging and drug delivery. *Curr. Opin. Chem. Biol.* **2012**, *16*, 429–435.
- (24) Funai, T.; Miyazaki, Y.; Aotani, M.; Yamaguchi, E.; Nakagawa, O.; Wada, S.-I.; Torigoe, H.; Ono, A.; Urata, H. AgI Ion Mediated Formation of a C–A Mispair by DNA Polymerases. *Angew. Chem., Int. Ed.* **2012**, *51*, 6464–6466.
- (25) Funai, T.; Nakamura, J.; Miyazaki, Y.; Kiriu, R.; Nakagawa, O.; Wada, S.-I.; Ono, A.; Urata, H. Regulated Incorporation of Two Different Metal Ions into Programmed Sites in a Duplex by DNA Polymerase Catalyzed Primer Extension. *Angew. Chem., Int. Ed.* **2014**, *53*, *6624*–*6627*.
- (26) Clever, G. H.; Reitmeier, S. J.; Carell, T.; Schiemann, O. Antiferromagnetic Coupling of Stacked CuII—Salen Complexes in DNA. *Angew. Chem., Int. Ed.* **2010**, *49*, 4927—4929.
- (27) Mallajosyula, S. S.; Pati, S. K. Conformational Tuning of Magnetic Interactions in Metal–DNA Complexes. *Angew. Chem., Int. Ed.* **2009**, *48*, 4977–4981.
- (28) Tanaka, K.; Tengeiji, A.; Kato, T.; Toyama, N.; Shionoya, M. A Discrete Self-Assembled Metal Array in Artificial DNA. *Science* **2003**, 299, 1212–1213.
- (29) Carell, T.; Behrens, C.; Gierlich, J. Electrontransfer through DNA and metal-containing DNA. *Org. Biomol. Chem.* **2003**, *1*, 2221–2228.
- (30) Ito, T.; Nikaido, G.; Nishimoto, S.-I. Effects of metal binding to mismatched base pairs on DNA-mediated charge transfer. *J. Inorg. Biochem.* **2007**, *101*, 1090–1093.
- (31) Joseph, J.; Schuster, G. B. Long-Distance Radical Cation Hopping in DNA: The Effect of Thymine–Hg(II)–Thymine Base Pairs. *Org. Lett.* **200**7, *9*, 1843–1846.
- (32) Katz, S. The reversible reaction of Hg (II) and double-stranded polynucleotides a step-function theory and its significance. *Biochim. Biophys. Acta, Spec. Sect. Nucleic Acids Relat. Subj.* **1963**, *68*, 240–253.
- (33) Yamaguchi, H.; Šebera, J.; Kondo, J.; Oda, S.; Komuro, T.; Kawamura, T.; Dairaku, T.; Kondo, Y.; Okamoto, I.; Ono, A.; Burda, J. V.; Kojima, C.; Sychrovský, V.; Tanaka, Y. The structure of metallo-DNA with consecutive thymine—Hg<sup>II</sup>—thymine base pairs explains positive entropy for the metallo base pair formation. *Nucleic Acids Res.* **2013**, *42*, 4094–4099.
- (34) Liu, H.; Shen, F.; Haruehanroengra, P.; Yao, Q.; Cheng, Y.; Chen, Y.; Yang, C.; Zhang, J.; Wu, B.; Luo, Q.; Cui, R.; Li, J.; Ma, J.; Sheng, J.; Gan, J. A DNA Structure Containing AgI-Mediated G:G and C:C Base Pairs. *Angew. Chem., Int. Ed.* **2017**, *56*, 9430–9434.
- (35) Izatt, R. M.; Christensen, J. J.; Rytting, J. H. Sites and thermodynamic quantities associated with proton and metal ion

- interaction with ribonucleic acid, deoxyribonucleic acid, and their constituent bases, nucleosides, and and nucleotides. *Chem. Rev.* **1971**, 71, 439–481.
- (36) Takezawa, Y.; Shionoya, M. Metal-Mediated DNA Base Pairing: Alternatives to Hydrogen-Bonded Watson-Crick Base Pairs. Acc. Chem. Res. 2012, 45, 2066–2076.
- (37) Nolan, E. M.; Lippard, S. J. Tools and Tactics for the Optical Detection of Mercuric Ion. *Chem. Rev.* **2008**, *108*, 3443–3480.
- (38) Ono, A.; Togashi, H. Highly Selective Oligonucleotide-Based Sensor for Mercury(II) in Aqueous Solutions. *Angew. Chem., Int. Ed.* **2004**, *43*, 4300–4302.
- (39) Song, Y.; Wei, W.; Qu, X. Colorimetric Biosensing Using Smart Materials. *Adv. Mater.* **2011**, 23, 4215–4236.
- (40) Copp, S. M.; Swasey, S. M.; Gorovits, A.; Bogdanov, P.; Gwinn, E. G. General Approach for Machine Learning-Aided Design of DNA-Stabilized Silver Clusters. *Chem. Mater.* **2020**, *32*, 430–437.
- (41) Davies, B. P.; Arenz, C. A fluorescence probe for assaying micro RNA maturation. *Bioorg. Med. Chem.* **2008**, *16*, 49–55.
- (42) Larkey, N. E.; Almlie, C. K.; Tran, V.; Egan, M.; Burrows, S. M. Detection of miRNA Using a Double-Strand Displacement Biosensor with a Self-Complementary Fluorescent Reporter. *Anal. Chem.* **2014**, *86*, 1853–1863.
- (43) Lakowicz, J. R. Principles of fluorescence spectroscopy; Springer science & business media: 2013; pp. 368–391.
- (44) Aramendia, P. F.; Negri, R. M.; Roman, E. S. Temperature Dependence of Fluorescence and Photoisomerization in Symmetric Carbocyanines.Influence of Medium Viscosity and Molecular Structure. *J.Phys. Chem.* **1994**, *98*, 3165–3173.
- (45) Torigoe, H.; Okamoto, I.; Dairaku, T.; Tanaka, Y.; Ono, A.; Kozasa, T. Thermodynamic and structural properties of the specific binding between Ag<sup>+</sup> ion and C:C mismatched base pair in duplex DNA to form C-Ag-C metal-mediated base pair. *Biochimie* **2012**, *94*, 2431–2440.
- (46) Swasey, S. M.; Leal, L. E.; Lopez-Acevedo, O.; Pavlovich, J.; Gwinn, E. G. Silver (I) as DNA glue: Ag<sup>+</sup>—mediated guanine pairing revealed by removing Watson-Crick constraints. *Sci. Rep.* **2015**, *S*, 10163.